A Molecular Tetrad Allowing Efficient Energy Storage for 1.6 s at 163 K

7 AUTHORS, INCLUDING:

Yukiyasu Kashiwagi
Osaka Municipal Technical Research Institute
40 PUBLICATIONS **1,388** CITATIONS

Hiroko Yamada
Nara Institute of Science and Technology
156 PUBLICATIONS **3,893** CITATIONS

A Molecular Tetrad Allowing Efficient Energy Storage for 1.6 s at 163 K

Dirk M. Guldi,*,† Hiroshi Imahori,*,‡ Koichi Tamaki,§ Yukiyasu Kashiwagi,|| Hiroko Yamada,|| Yoshiteru Sakata,§ and Shunichi Fukuzumi*,||

Radiation Laboratory, University of Notre Dame, Notre Dame, Indiana 46556, Department of Molecular Engineering, Graduate School of Engineering, Kyoto University, PRESTO, Japan Science and Technology Agency (JST), Katsura, Nishikyo-ku, Kyoto 615-8510, Fukui Institute for Fundamental Chemistry, Kyoto University, 34-4, Takano-Nishihiraki-cho, Sakyo-ku, Kyoto 606-8103, The Institute of Scientific and Industrial Research, Osaka University, Mihoga-oka, Ibaraki, Osaka 567-0047, and Department of Material and Life Science, Graduate School of Engineering, Osaka University, CREST, JST, Suita, Osaka 565-0871, Japan

In a novel molecular ferrocene−zinc porphyrin−zinc porphyrin−fullerene (Fc−ZnP−ZnP−C_{60}) tetrad, the longest lifetime of a charge-separated state ever reported in an artificial photosynthetic reaction center (1.6 s in DMF at 163 K) has been attained. This lifetime is comparable, for example, to the lifetime (∼1 s) of the bacteriochlorophyll dimer radical cation $((Bchl)_2^{\bullet+})$−secondary quinone radical anion $(Q_B^{\bullet-})$ ion pair in the bacterial photosynthetic reaction centers. The present far distant radical ion pair is formed with a quantum yield of 34%. The radical ion pair Fc$^+$−ZnP−ZnP−$C_{60}^{\bullet-}$ produced by photoinduced electron transfer was detected by means of transient absorption spectra as well as ESR spectra. Both the lifetime and the quantum yield of the final charge-separated state are improved in Fc−ZnP−ZnP−C_{60} relative to the corresponding ferrocene−zinc porphyrin−free base porphyrin−fullerene (Fc−ZnP−H_2P−C_{60}) tetrad.

Introduction

The most effective strategy to achieve long-distance, charge-separated states makes use of a sequence of several short-range electron-transfer reactions along well-designed redox gradients.[1−7] The natural photosynthetic reaction center executes this process with maximum productivity, separating charges with unit efficiency to yield a spatially and also electronically well-isolated radical ion pair.[8]

The recent reported efficiency of 24% found for a long-distance radical pair in a molecular tetrad (i.e., Fc−ZnP−H_2P−C_{60}; see Chart 1) is a promising starting point.[9] Despite the fact that the small reorganization energy of fullerenes in electron-transfer reactions assists—among many other factors—in accelerating the crucial charge-separation step,[10−19] the free energy changes of electron transfer for the formation of initial Fc−ZnP−H_2P$^{\bullet+}$−$C_{60}^{\bullet-}$ ($^1H_2$P*, $-\Delta G°_{ET(CS)} = 0.26$ eV; $^1C_{60}$*, $-\Delta G°_{ET(CS)} = 0.12$ eV; in benzonitrile (PhCN)) are, nevertheless, far away from being optimized. Optimal conditions are, for example, a free energy change of reaction ($-\Delta G°_{ET(CS)}$) close to the thermodynamic maximum, which equals the reorganization energy ($-\Delta G°_{ET(CS)} \approx \lambda$).[20]

Further advances involve substitution of the metal-free tetraphenylporphyrin chromophore (H_2P) by the corresponding zinc analogue (ZnP).[21] The advantage of this approach is 2-fold: First, it raises the excited-state energy of the chromophore from approximately 1.89 to 2.04 eV. Second, it lowers the oxidation potential of the electron donor by nearly 300 mV.

As a consequence of these two effects, the energy gap of the initial charge-separation step is markedly widened ($-\Delta G°_{ET(CS)} = 0.66$ eV in PhCN), which should ensure a better efficiency, besides being closer to the thermodynamic maximum (i.e., λ for ZnP−C_{60} is ca. 0.7 eV[9,20]).

We report herein on a molecular tetrad, ferrocene−zinc porphyrin−zinc porphyrin−fullerene (Fc−ZnP−ZnP−C_{60}), a promising model system that stores 1.1 eV of the initial excitation energy for 1.6 s at 163 K. Most importantly, the quantum yield of forming the far distant radical ion pair is 34%, which is improved compared to that of ferrocene−zinc porphyrin−free base porphyrin−fullerene (Fc−ZnP−H_2P−C_{60}).

Experimental Section

General Procedures. Melting points were recorded on a Yanagimoto micro melting point apparatus and not corrected. ^{1}H NMR spectra were measured on a JEOL EX-270 or a JEOL JNM-LA400 using tetramethylsilane as internal standard. Fast atom bombardment (FAB) mass spectra were obtained on a JEOL JMS-DX300. Matrix-assisted laser desorption/ionization (MALDI) time-of-flight (TOF) mass spectra were measured on a Kratos Compact MALDI I (Shimadzu). Steady-state absorption spectra were measured on a Shimadzu UV3000 spectrometer. Fluorescence spectra were taken using a SPEX FluoroMAX-2 fluorometer and corrected. The edge-to-edge distances (R_{ee}) were determined from CPK modeling using CAChe (version 3.7 CAChe Scientific, 1994).

Materials. All solvents and chemicals were of reagent grade quality, obtained commercially and used without further purification except as noted below. Tetrabutylammonium hexafluorophosphate, used as a supporting electrolyte for the electrochemical measurements, was obtained from Tokyo Kasei Organic Chemicals. THF, PhCN, and DMF were purchased from Wako Pure Chemical Industries, Ltd. and purified by

* To whom correspondence should be addressed. E-mail: guldi.1@nd.edu (D.M.G.); imahori@scl.kyoto-u.ac.jp (H.I.); fukuzumi@ap.chem.eng.osaka-u.ac.jp (S.F.).
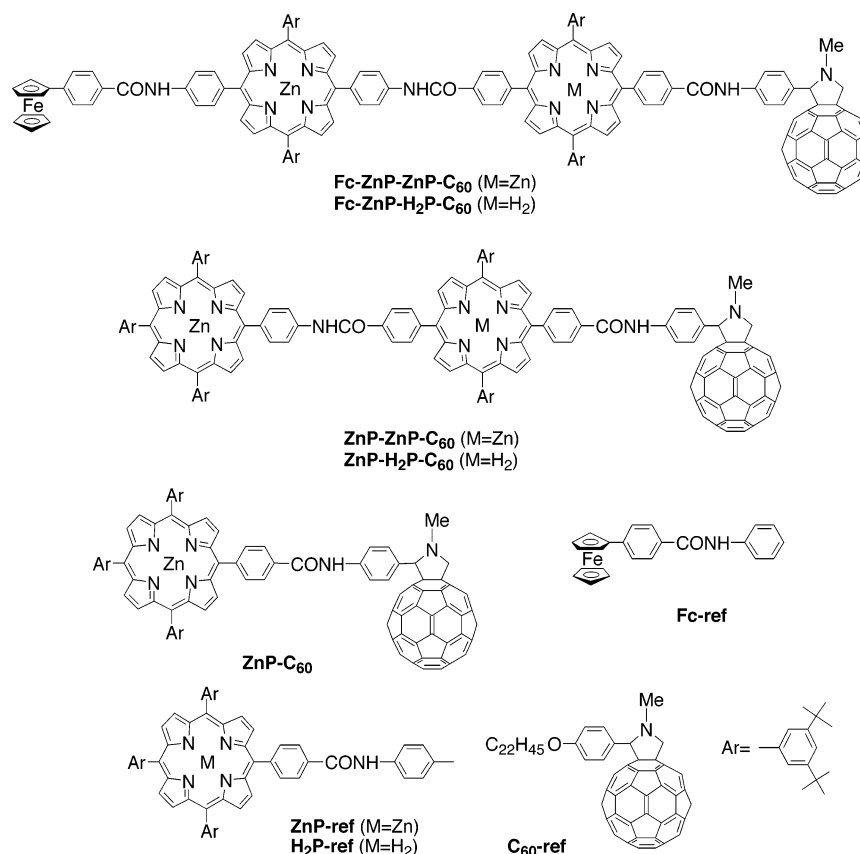
† University of Notre Dame.

‡ Graduate School of Engineering and Fukui Institute for Fundamental Chemistry, Kyoto University.

§ The Institute of Scientific and Industrial Research, Osaka University.

|| Graduate School of Engineering, Osaka University.

CHART 1

Fc-ZnP-ZnP-C$_{60}$ (M=Zn)
Fc-ZnP-H$_2$P-C$_{60}$ (M=H$_2$)

ZnP-ZnP-C$_{60}$ (M=Zn)
ZnP-H$_2$P-C$_{60}$ (M=H$_2$)

ZnP-C$_{60}$

Fc-ref

ZnP-ref (M=Zn)
H$_2$P-ref (M=H$_2$)

C$_{60}$-ref

successive distillation over calcium hydride. Thin-layer chromatography (TLC) and flash column chromatography were performed with Art. 5554 DC-Alufolien Kieselgel 60 F$_{254}$ (Merck) and Fujisilicia BW300, respectively.

Synthesis of Fc−ZnP−ZnP−C$_{60}$. A saturated methanol solution of Zn(OAc)$_2$ (3.6 mL) was added to a solution of Fc−ZnP−H$_2$P−C$_{60}$[9] (28.0 mg, 0.00939 mmol) in CHCl$_3$ (150 mL) and heated at reflux for 30 min. After cooling, the reaction mixture was washed with saturated NaHCO$_3$ aqueous solution twice and dried over anhydrous Na$_2$SO$_4$, and then the solvent was evaporated. Flash column chromatography on silica gel with CS$_2$:CHCl$_3$:THF = 4:16:1 as an eluent (R_f = 0.30) and subsequent reprecipitation from THF−methanol gave Fc−ZnP−ZnP−C$_{60}$ as a dark violet solid (98% yield, 28.0 mg, 0.00939 mmol): mp > 300 °C; ^{1}H NMR (400 MHz, CDCl$_2$CDCl$_2$ + pyridine-d_5, 60 °C) δ 1.56 (s, 72H), 2.88 (s, 3H), 4.12 (s, 5H), 4.29 (d, J = 10 Hz, 1H), 4.45 (s, 2H), 4.79 (s, 2H), 4.99 (s, 1H), 5.00 (d, J = 10 Hz, 1H), 7.6−8.6 (m, 39H), 8.8−9.1 (m, 16H); MALDI-TOF MS m/z 3045 (M + H$^+$), calcd for C$_{208}$H$_{142}$N$_{12}$FeO$_3$Zn$_2$ 3044.0.

Synthesis of ZnP−ZnP−C$_{60}$. A saturated methanol solution of Zn(OAc)$_2$ (0.5 mL) was added to a solution of ZnP−H$_2$P−C$_{60}$[22] (8.5 mg, 3.0 mmol) in CHCl$_3$ (20 mL) and heated at reflux for 30 min. After cooling, the reaction mixture was washed with water twice and dried over anhydrous Na$_2$SO$_4$, and then the solvent was evaporated. Flash column chromatography on silica gel with CHCl$_3$ as an eluent and subsequent reprecipitation from chloroform−methanol gave ZnP−ZnP−C$_{60}$ as a brown solid (6.8 mg, 2.3 mmol, 77%): mp > 300 °C; ^{1}H NMR (270 MHz, CDCl$_3$, 50 °C) δ 9.05 (d, J = 5 Hz, 2H), 9.0 (m, 10H), 8.96 (d, J = 5 Hz, 2H), 8.87 (d, J = 5 Hz, 2H), 8.56 (br, 2H), 8.43 (s, 4H), 8.31 (d, J = 8 Hz, 2H), 8.24 (m, 4H), 8.19 (d, J = 8 Hz, 2H), 8.10 (m, 6H), 8.06 (d, J = 2 Hz, 4H), 7.93 (d, J =

8 Hz, 2H), 7.81 (m, 5H), 7.68 (d, J = 9 Hz, 2H), 4.60 (d, J = 9 Hz, 1H), 4.47 (s, 1H), 3.83 (d, J = 8 Hz, 1H), 2.72 (s, 3H), 1.54 (s, 54H), 1.53 (s, 36H); MALDI-TOF MS m/z 2854 (M + H$^+$), calcd for C$_{199}$H$_{145}$N$_{11}$O$_2$Zn$_2$ 2853.0.

Electrochemical Measurements. The differential pulse voltammetry measurements were performed on a BAS 50W electrochemical analyzer in a deaerated PhCN (or THF and DMF) solution containing 0.10 M n-Bu$_4$NPF$_6$ as a supporting electrolyte at 298 K (10 mV s^{-1}). The glassy carbon working electrode was polished with BAS polishing alumina suspension and rinsed with acetone before use. The counter electrode was a platinum wire. The measured potentials were recorded with respect to a Ag/AgCl (saturated KCl) reference electrode. Ferrocene/ferricenium was used as an external standard.[9]

Flash Photolysis Experiments. For flash photolysis studies, the fullerene concentrations were prepared to exhibit an optical density of at least 0.02 at 532 nm, the wavelength of irradiation. Picosecond laser flash photolysis experiments were carried out with 532 nm laser pulses from a mode-locked, Q-switched Quantel YG-501 DP Nd:YAG laser system (pulse width ∼18 ps, 2−3 mJ/pulse). The white continuum picosecond probe pulse was generated by passing the fundamental output through a D$_2$O/H$_2$O solution. Nano- to millisecond laser flash photolysis experiments were performed with laser pulses from a Quanta-Ray CDR Nd:YAG system (532 nm, 6 ns pulse width) in a front face excitation geometry. A Xe lamp was triggered synchronously with the laser. A monochromator (SPEX) in combination with either a Hamamatsu R 5108 photomultiplier or a fast InGaAs diode was employed to monitor transient absorption spectra. The quantum yields were measured using the comparative method. In particular, the strong fullerene triplet−triplet absorption ($\epsilon_{700\ nm}$ = 16100 M^{-1} cm^{-1}; $\Phi_{TRIPLET}$ = 0.98)[22] served as a probe to obtain the quantum yields for the charge-

Molecular Tetrad Allowing Energy Storage for 1.6 s

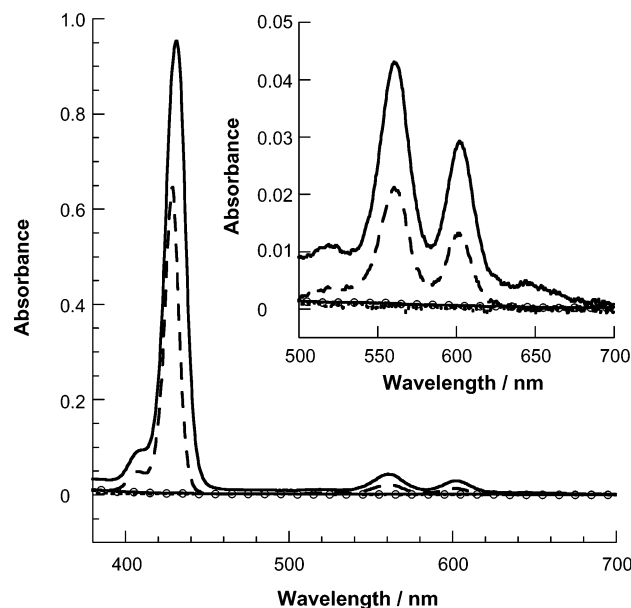*J. Phys. Chem. A, Vol. 108, No. 4, 2004* **543**

Figure 1. Absorption spectra of Fc−ZnP−ZnP−C_{60} (solid line), Fe-ref (dotted line), ZnP-ref (dashed line), and C_{60}-ref (solid line with circles) in DMF (1.0×10^{-6} M).

Figure 2. Fluorescence spectra of Fc−ZnP−ZnP−C_{60} (solid line) and ZnP-ref (dotted line) in PhCN when adjusting to the same absorbance at the 431 nm excitation wavelength.

separated state, especially for the fullerene π-radical anion ($\epsilon_{1000\,nm} = 4700$ M^{-1} cm^{-1}).[22] Solutions of the C_{60}-reference and the donor−acceptor ensemble were prepared to exhibit identical absorptions at the excitation wavelength—532 nm. Then, differential absorption changes (ΔOD) were measured at 700 and 1000 nm, respectively. By probing samples with absorptions in the range between 0.05 and 0.5, possible filter effects were eliminated and the linearity of the response was guaranteed.

ESR Measurements under Photoirradiation. A quartz ESR tube (internal diameter 4.5 mm) containing deaerated PhCN solutions of the porphyrin−fullerene linked compounds (1.0×10^{-5} M) was irradiated in the cavity of the ESR spectrometer with the focused light of a 1000 W high-pressure Hg lamp (Ushio-USH1005D) through an aqueous filter. The internal diameter of the ESR tube is 4.5 mm, which is small enough to fill the ESR cavity, but large enough to obtain good signal-to-noise ratios during the ESR measurements under photoirradiation at low temperatures. The ESR spectra in frozen PhCN were measured under nonsaturating microwave power conditions at various temperatures (163−203 K) with a JEOL X-band spectrometer (JES-RE1XE) using an attached variable-temperature apparatus.[9]

Results and Discussion

Synthesis. The synthesis and characterization of Fc−ZnP−H$_2$P−C_{60},[9] ZnP−H$_2$P−C_{60},[22] ZnP−C_{60},[22] ZnP-ref,[22] H$_2$P-ref,[22] Fc-ref,[9] and C_{60}-ref[9] (Chart 1) have been described previously. Fc−ZnP−ZnP−C_{60} and ZnP−ZnP−C_{60} were obtained by treatment of Fc−ZnP−H$_2$P−C_{60} and ZnP−H$_2$P−C_{60} with zinc acetate, respectively (Chart 1). Structures of all new compounds were confirmed by spectroscopic analysis including ^{1}H NMR and MALDI-TOF mass spectra (see the Experimental Section).

Absorption and Fluorescence Spectra. Figure 1 displays the absorption spectra of Fc−ZnP−ZnP−C_{60}, Fc-ref, ZnP-ref, and C_{60}-ref in DMF. The absorption features of the two zinc porphyrin moieties in the visible region are much stronger than those of the ferrocene and the C_{60} moieties, which allows us to excite the zinc porphyrin moiety selectively with 532 nm light. It should be noted here that the Soret band of Fc−ZnP−ZnP−
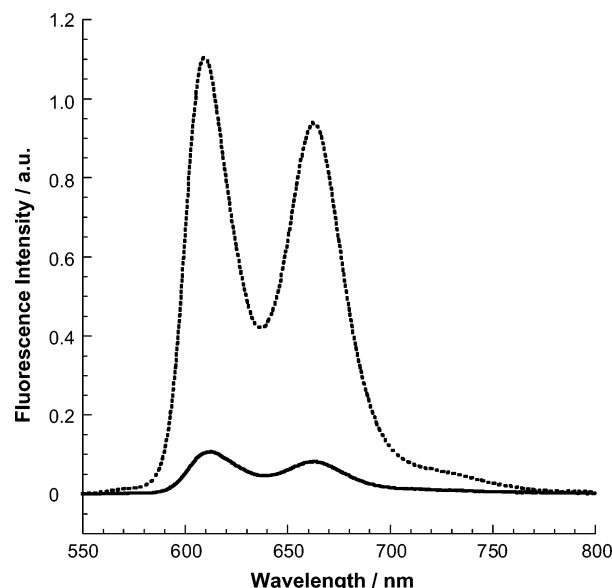
TABLE 1: One-Electron Redox Potentials (versus Fc/Fc$^+$)^a of Fc−ZnP−ZnP−C_{60}, ZnP-ref, Fc-ref, and C_{60}-ref in Various Solvents

		$E°_{ox}$/V		$E°_{red}$/V
compound	solvent	ZnP$^{•+}$/ZnP	Fc$^+$/Fc	C_{60}/$C_{60}^{•-}$
Fc−ZnP−ZnP−C_{60}	PhCN	0.31	0.07	−1.04
ZnP-ref, Fc-ref, C_{60}-ref	THF	0.40^b	0.05^b	−1.02^b
ZnP-ref, Fc-ref, C_{60}-ref	PhCN	0.34^b	0.07^b	−1.04^b
ZnP-ref, Fc-ref, C_{60}-ref	DMF	0.29^b	0.06^b	−0.92^b

^{a} The redox potentials were measured by differential pulse voltammetry in THF, PhCN, and DMF using 0.10 M n-Bu$_4$NPF$_6$ as a supporting electrolyte with a sweep rate of 10 mV s^{-1}. ^{b} Taken from ref 9.

C_{60} (431 nm) becomes broad and is slightly red-shifted by 2 nm as compared to that of ZnP-ref (429 nm). This indicates a small contribution of the exciton coupling in the zinc porphyrin dimer with a rigid spacer.[3b] Similar spectra were found in THF and PhCN.

Steady-state fluorescence spectra of Fc−ZnP−ZnP−C_{60}, ZnP−ZnP−C_{60}, and ZnP−C_{60} in PhCN match that of ZnP-ref ($\lambda_{em}^{max} = 609$, 663 nm). After the relative absorbance at the 431 nm excitation wavelength is adjusted, the fluorescence spectra of Fc−ZnP−ZnP−C_{60}, ZnP−ZnP−C_{60}, and ZnP−C_{60} in PhCN indicate quenching relative to ZnP-ref (relative intensities 0.10 for Fc−ZnP−ZnP−C_{60}, 0.10 for ZnP−ZnP−C_{60}, 0.04 for ZnP−C_{60}, and 1 for ZnP-ref). An illustration is given in Figure 2 in which the fluorescence spectra of Fc−ZnP−ZnP−C_{60} and ZnP-ref are compared. The fluorescence quenching is attributed to intramolecular photoinduced ET from the singlet excited state of ZnP to C_{60} (vide infra).

One-Electron Redox Potentials and ET Driving Force. An accurate determination of the driving force ($-\Delta G°_{ET}$) for all the *intra*molecular ET processes required measuring the redox potentials of Fc−ZnP−ZnP−C_{60} and the reference chromophores (Fc-ref, ZnP-ref, and C_{60}-ref) in various solvents. The differential pulse voltammetry was performed in THF, PhCN, and DMF solutions containing the same supporting electrolyte (i.e., 0.10 M n-Bu$_4$NPF$_6$). Table 1 summarizes all the redox potentials of the investigated compounds. The first one-electron oxidation potentials ($E°_{ox}$) of ZnP-ref (0.34 V vs ferrocene/

ferricenium (Fc/Fc$^+$)) and Fc-ref (0.07 V vs Fc/Fc$^+$) and first one-electron reduction potential ($E°_{red}$) of C$_{60}$-ref (-1.04 V vs Fc/Fc$^+$) in PhCN are virtually the same as those of Fc$-$ZnP$-$ZnP$-$C$_{60}$ in PhCN. This implies that electronic interaction between the chromophores is negligible in the ground state. The first one-electron oxidation potential of Fc-ref remains nearly constant, despite the substantial increase in solvent polarity. On the other hand, ZnP-ref and C$_{60}$-ref exhibit negative and positive shifts, respectively, for the underlying first one-electron oxidation and reduction potentials with increasing solvent polarity. The one-electron reduction potentials of reference compounds ZnP-ref and H$_2$P-ref were also determined as -1.82 V[21] and -1.64 V in PhCN (vs Fc/Fc$^+$), respectively. This indicates that the LUMO energy of ZnP-ref is higher than that of H$_2$P-ref.

The driving forces ($-\Delta G°_{ET(CR)}$) for the intramolecular charge-recombination processes from the fullerene radical anion (C$_{60}$$^{•-}$) to the zinc porphyrin radical cation (ZnP$^{•+}$) and the ferricenium ion (Fc$^+$) were calculated by eq 1, where e stands

$$-\Delta G°_{ET(CR)} = e[E°_{ox}(D^{•+}/D) - E°_{red}(A/A^{•-})] \quad (1)$$

for the elementary charge. On the other hand, the driving forces for the intramolecular charge-separation processes ($-\Delta G°_{ET(CS)}$) from the zinc porphyrin singlet excited state to C$_{60}$ was determined by eq 2, where ΔE_{0-0} represents the energy of the

$$-\Delta G°_{ET(CS)} = \Delta E_{0-0} + \Delta G°_{ET(CR)} \quad (2)$$

0$-$0 energy gap between the lowest excited singlet state and the ground state, which is determined by the 0$-$0* absorption and 0*$-$0 fluorescence maxima. The driving forces for intramolecular charge-shift (CSH) processes ($-\Delta G°_{ET(CSH)}$) from the Fc to the ZnP$^{•+}$ in Fc$-$ZnP$-$ZnP$-$C$_{60}$ were determined by subtracting the energy of the final state from that of the initial state.

Photodynamical Studies. We reported previously the photodynamics of ZnP$-$C$_{60}$, ZnP$-$H$_2$P$-$C$_{60}$, Fc$-$ZnP$-$C$_{60}$, and Fc$-$ZnP$-$H$_2$P$-$C$_{60}$ in PhCN in depth.[9,21,22] Herein we focus on the photodynamics of ZnP$-$ZnP$-$C$_{60}$ and Fc$-$ZnP$-$ZnP$-$C$_{60}$ in comparison with those of preciously reported dyad, triad, and tetrad systems.[9,21,22]

ZnP$-$ZnP$-$C$_{60}$ Triad. Pumping light into the ZnP ground state with short 532 nm laser pulses (i.e., absorption ratio ZnP:C$_{60}$ = 85:15) led to the population of its singlet excited state, ^{1}ZnP*. The lifetime of this intermediate state is short, since the lowest vibrational state of the singlet excited state undergoes efficient charge separation to yield ZnP$-$ZnP$^{•+}$$-C_{60}$$^{•-}$. Spectral characteristics of the charge-separated state of ZnP$-$ZnP$-$C$_{60}$ comprise transient absorption in the visible and near-infrared with characteristic maxima around 650 nm (i.e., ZnP$^{•+}$) and 1000 nm (i.e., C$_{60}$$^{•-}$), respectively, similar to that found for ZnP$-$C$_{60}$ as shown in Figure 3. In deoxygenated PhCN, for example, charge separation takes place with a time constant of 1.1×10^{10} s^{-1}.

The lifetime of the radical ion pair in ZnP$-$ZnP$-$C$_{60}$ reveals a two-component decay as shown in Figure 4. The faster segment (Figure 4a) reveals a lifetime of several hundred nanoseconds, while the slower segment (Figure 4b) lies in the range of several tens of microseconds; see Table 2. Both decay components were best fitted by first-order kinetics. This leads us to conclude that both processes are intramolecular in nature. What is interesting to note is that not only are the decay rates of the short-lived species identical with those of ZnP$^{•+}$$-C_{60}$$^{•-}$ in the dyad (Table 2), but also their spectral characteristics are
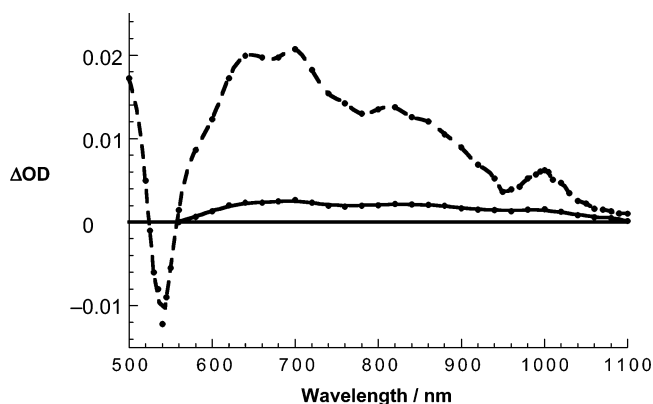

Figure 3. Differential absorption changes recorded 50 ns (dashed line) and 4 μs (solid line) after 532 nm excitation of ZnP$-$ZnP$-$C$_{60}$ (1.0 $\times$ 10^{-5} M) in deaerated PhCN solution.
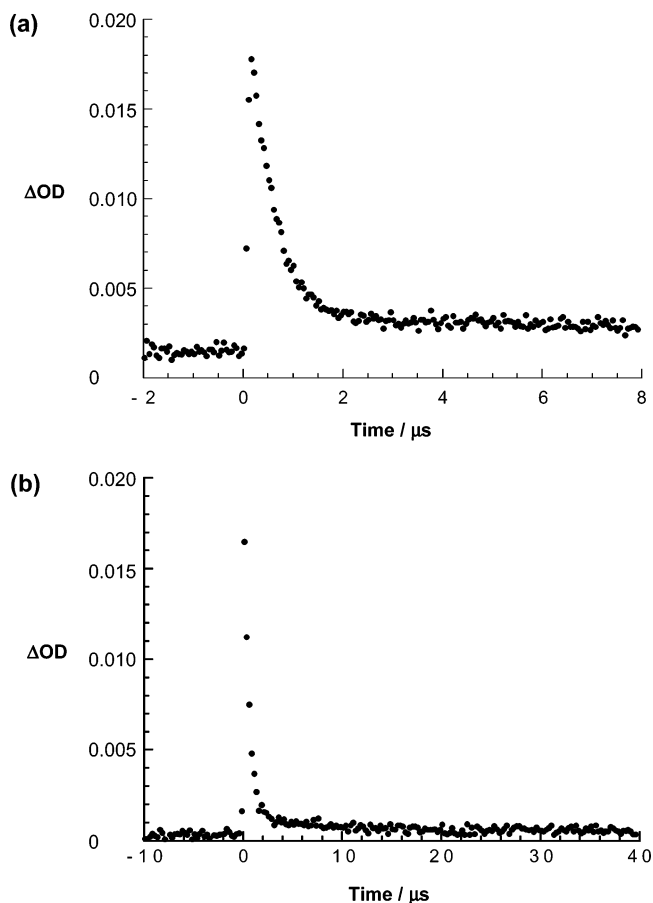

Figure 4. Time$-$absorption profiles recorded at 1000 nm after 532 nm excitation of ZnP$-$ZnP$-$C$_{60}$ (1.0 $\times$ 10^{-5} M) (a) up to 8 μs and (b) up to 40 μs in deaerated PhCN solution.

superimposable. On the basis of these kinetic and spectroscopic accounts, we must infer that the origin of this fast decay process is the adjacent radical ion pair, ZnP$-$ZnP$^{•+}$$-C_{60}$$^{•-}$. Taking into account the similarity in molecular structure of ZnP$-$ZnP$-$C$_{60}$ and ZnP$-$H$_2$P$-$C$_{60}$, the lifetimes of ZnP$^{•+}$$-H_2P-C_{60}$$^{•-}$ (PhCN, 21 μs) helped to shed light on the nature of the secondary component. The close match between them leads us to postulate that the long-lived product is the distant radical ion pair, namely, ZnP$^{•+}$$-ZnP-C_{60}$$^{•-}$. Thus, the coupling between the two zinc porphyrins$-$in the central ZnP$-$ZnP building block$-$is sufficient to create the far distant analogue to ZnP$-$ZnP$^{•+}$$-C_{60}$$^{•-}$, that is, ZnP$^{•+}$$-ZnP-C_{60}$$^{•-}$ via an intramolecular charge-shift reaction.[25-27]

Molecular Tetrad Allowing Energy Storage for 1.6 s

J. Phys. Chem. A, Vol. 108, No. 4, 2004 **545**

TABLE 2: Rate Constants (k_{ET}) for Charge Separation (CS) and Charge Recombination (CR) and the Free Energy Changes ($-\Delta G°_{ET}$) in the ZnP−ZnP−C$_{60}$ Triad at 298 K

solvent	initial state[a]	final state[a]	$-\Delta G°_{ET}$/eV	k/s^{-1}	Φ_{CS}(total)
THF ($\epsilon_s = 7.58$)	ZnP−^{1}ZnP*−C$_{60}$ (2.07 eV)	ZnP−ZnP$^{•+}$−C$_{60}^{•-}$ (1.42 eV)	0.65	$k_{ET(CS1)} = 1.1 \times 10^{10}$	
	ZnP−ZnP$^{•+}$−C$_{60}^{•-}$ (1.42 eV)	ZnP−ZnP−C$_{60}$	1.42		0.74
	ZnP$^{•+}$−ZnP−C$_{60}^{•-}$ (1.42 eV)	ZnP−ZnP−C$_{60}$	1.42	$k_{ET(CR2)} = 3.0 \times 10^4$	0.06
PhCN ($\epsilon_s = 25.2$)	ZnP−^{1}ZnP*−C$_{60}$ (2.04 eV)	ZnP−ZnP$^{•+}$−C$_{60}^{•-}$ (1.38 eV)	0.66	$k_{ET(CS1)} = 1.1 \times 10^{10}$	
	ZnP−ZnP$^{•+}$−C$_{60}^{•-}$ (1.38 eV)	ZnP−ZnP−C$_{60}$	1.38	$k_{ET(CR1)} = 1.2 \times 10^6$	0.85
	ZnP$^{•+}$−ZnP−C$_{60}^{•-}$ (1.38 eV)	ZnP−ZnP−C$_{60}$	1.38	$k_{ET(CR2)} = 6.6 \times 10^4$	0.05
DMF ($\epsilon_s = 36.7$)	ZnP−^{1}ZnP*−C$_{60}$ (2.06 eV)	ZnP−ZnP$^{•+}$−C$_{60}^{•-}$ (1.21 eV)	0.85	$k_{ET(CS1)} = 1.4 \times 10^{10}$	
	ZnP−ZnP$^{•+}$−C$_{60}^{•-}$ (1.21 eV)	ZnP−ZnP−C$_{60}$	1.21	$k_{ET(CR1)} = 1.6 \times 10^6$	0.50
	ZnP$^{•+}$−ZnP−C$_{60}^{•-}$ (1.21 eV)	ZnP−ZnP−C$_{60}$	1.21	$k_{ET(CR2)} = 5.0 \times 10^4$	0.05

[a] The energy of each state relative to the ground state is given in parentheses.

TABLE 3: Rate Constants (k_{ET}) for CS and CR and the Free Energy Changes ($-\Delta G°_{ET}$) in the Fc−ZnP−ZnP−C$_{60}$ Tetrad at 298 K

solvent	initial state[a]	final state[a]	$-\Delta G°_{ET}$/eV	k/s^{-1}	Φ_{CS}(total)
THF ($\epsilon_s = 7.58$)	Fc−ZnP−^{1}ZnP*−C$_{60}$ (2.07 eV)	Fc−ZnP−ZnP$^{•+}$−C$_{60}^{•-}$ (1.42 eV)	0.65	$k_{ET(CS1)} = 1.2 \times 10^{10}$	
	Fc−ZnP$^{•+}$−ZnP−C$_{60}^{•-}$ (1.42 eV)	Fc$^+$−ZnP−ZnP−C$_{60}^{•-}$ (1.07 eV)	0.35	$k_{ET(CSH2)} = 7.6 \times 10^8$	
	Fc$^+$−ZnP−ZnP−C$_{60}^{•-}$ (1.07 eV)	Fc−ZnP−ZnP−C$_{60}$	1.07		0.26
PhCN ($\epsilon_s = 25.2$)	Fc−ZnP−^{1}ZnP*−C$_{60}$ (2.04 eV)	Fc−ZnP−ZnP$^{•+}$−C$_{60}^{•-}$ (1.38 eV)	0.66	$k_{ET(CS1)} = 1.3 \times 10^{10}$	
	Fc−ZnP$^{•+}$−ZnP−C$_{60}^{•-}$ (1.38 eV)	Fc$^+$−ZnP−ZnP−C$_{60}^{•-}$ (1.11 eV)	0.27	$k_{ET(CSH2)} = 8.1 \times 10^8$	
	Fc$^+$−ZnP−ZnP−C$_{60}^{•-}$ (1.11 eV)	Fc−ZnP−ZnP−C$_{60}$	1.11	$k_{ET(CR3)}{}^b = 0.76$	0.34
DMF ($\epsilon_s = 36.7$)	Fc−ZnP−^{1}ZnP*−C$_{60}$ (2.06 eV)	Fc−ZnP−ZnP$^{•+}$−C$_{60}^{•-}$ (1.21 eV)	0.85	$k_{ET(CS1)} = 1.3 \times 10^{10}$	
	Fc−ZnP$^{•+}$−ZnP−C$_{60}^{•-}$ (1.21 eV)	Fc$^+$−ZnP−ZnP−C$_{60}^{•-}$ (0.98 eV)	0.23	$k_{ET(CSH2)} = 8.1 \times 10^8$	
	Fc$^+$−ZnP−ZnP−C$_{60}^{•-}$ (0.98 eV)	Fc−ZnP−ZnP−C$_{60}$	0.98	$k_{ET(CR3)}{}^b = 0.64$	0.24

[a] The energy of each state relative to the ground state is given in parentheses. [b] Measured at 163 K.

Fc−ZnP−ZnP−C$_{60}$ Tetrad. Transient absorption measurements with Fc−ZnP−ZnP−C$_{60}$ in THF, PhCN, and DMF are similar to those in the aforementioned sections regarding the different ZnP−C$_{60}$ and ZnP−ZnP−C$_{60}$ ensembles. Upon 18 ps laser excitation of 1.0 × 10^{-5} M Fc−ZnP−ZnP−C$_{60}$ in deoxygenated solvents, the short-lived features of ^{1}ZnP*, that is, broad transitions in the 570−750 nm region, are still discernible. ^{1}ZnP* decays with rate constants of 1.2 × 10^{10}, 1.3 × 10^{10}, and 1.3 × 10^{10} s^{-1} in THF, PhCN, and DMF, respectively. A spectral comparison with ZnP$^{•+}$−C$_{60}^{•-}$ suggests that the product of these intramolecular reactions is the Fc−ZnP−ZnP$^{•+}$−C$_{60}^{•-}$ radical pair. This indicates that the photoinduced electron transfer occurs from Fc−ZnP−^{1}ZnP*−C$_{60}$ rather than from Fc−^{1}ZnP*−ZnP−C$_{60}$ to produce Fc−ZnP−ZnP$^{•+}$−C$_{60}^{•-}$. In addition, the one-electron-oxidized ZnP π-radical cation is readily identified by its broad maximum, located in the visible region around 650 nm. In contrast to the ZnP−C$_{60}$[21] and ZnP−ZnP−C$_{60}$ systems, the ZnP$^{•+}$ fingerprint is metastable and starts to decay already on the picosecond time scale, while the C$_{60}^{•-}$ absorption was found to be stable during this period. Taking the spectroscopic and kinetic evidence in concert and in accordance with our earlier work regarding Fc−ZnP−H$_2$P−C$_{60}$,[9] we assign the ZnP$^{•+}$ decay a charge shift from Fc to ZnP$^{•+}$, whose rate constants in the different media are listed in Table 3.[25]

In line with the proposed electron-transfer scenario, the differential absorption changes, recorded immediately after an 8 ns pulse, showed the same spectral features of C$_{60}^{•-}$ as observed at the end of the picosecond experiments. Specifically, two maxima located at 360 and 1000 nm were observed (Figure 5). Spectroscopically, the oxidized donor, Fc, can be identified by a weak absorption with an extinction coefficient of 1000 M^{-1} cm^{-1} at its 800 nm maximum.[28] The latter is, however, masked by the dominant features of C$_{60}^{•-}$. It should be noted that no absorption band due to the ZnP$^{•+}$ moiety (around 650 nm) is observed in the final charge-separated state of Fc−ZnP−ZnP−C$_{60}$ (Figure 5), in contrast with the case of ZnP−ZnP−C$_{60}$ (Figure 3). Scheme 1 sketches the reaction scheme and energy diagram for Fc−ZnP−ZnP−C$_{60}$ in PhCN. The C$_{60}^{•-}$
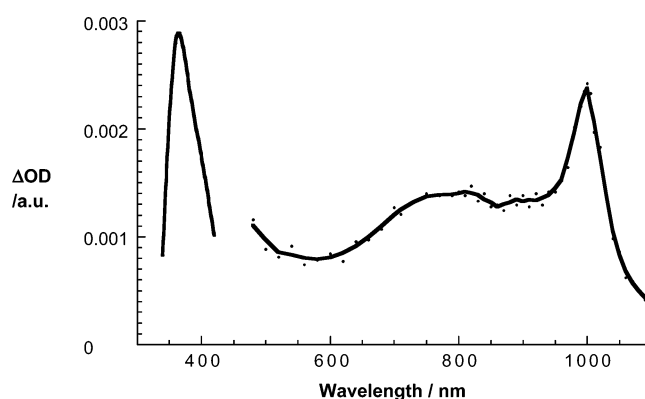

Figure 5. Differential absorption changes recorded 50 ns after 532 nm excitation of Fc−ZnP−ZnP−C$_{60}$ (1.0 × 10^{-5} M) in deaerated PhCN solution.

fingerprint allowed us to determine the lifetime of the final charge-separated state, Fc$^+$−ZnP−ZnP−C$_{60}^{•-}$. The decay curves (see the inset of Figure 6) were well fitted by bimolecular second-order kinetics (i.e., between two Fc$^+$−ZnP−ZnP−C$_{60}^{•-}$ molecules) rather than unimolecular first-order kinetics.[29] From the best fits *inter*molecular dynamics were calculated that are essentially diffusion controlled. In DMF the exact value is 1.8 × 10^9 M^{-1} s^{-1}, while using a highly viscous medium—Triton X-100—the rate was slowed to 5.0 × 10^8 M^{-1} s^{-1}.

To separate the intermolecular from the intramolecular processes in Fc$^+$−ZnP−ZnP−C$_{60}^{•-}$, electron spin resonance (ESR) measurements were performed in a frozen DMF or PhCN matrix at variable temperatures under irradiation. The use of a small concentration (1.0 × 10^{-5} M) of Fc−ZnP−ZnP−C$_{60}$ is essential to eliminate the contribution of intermolecular electron transfer between two Fc$^+$−ZnP−ZnP−C$_{60}^{•-}$ molecules to produce independent paramagnetic species, Fc$^+$−ZnP−ZnP−C$_{60}$ and Fc−ZnP−ZnP−C$_{60}^{•-}$, which have longer lifetimes than Fc$^+$−ZnP−ZnP−C$_{60}^{•-}$. The ESR spectrum in frozen DMF (Figure 7a) observed under irradiation at 163 K shows a characteristic isotropic signal attributable to a derivatized C$_{60}^{•-}$ (g = 2.0004).[30] The maximum slope line width (ΔH_{msl} =
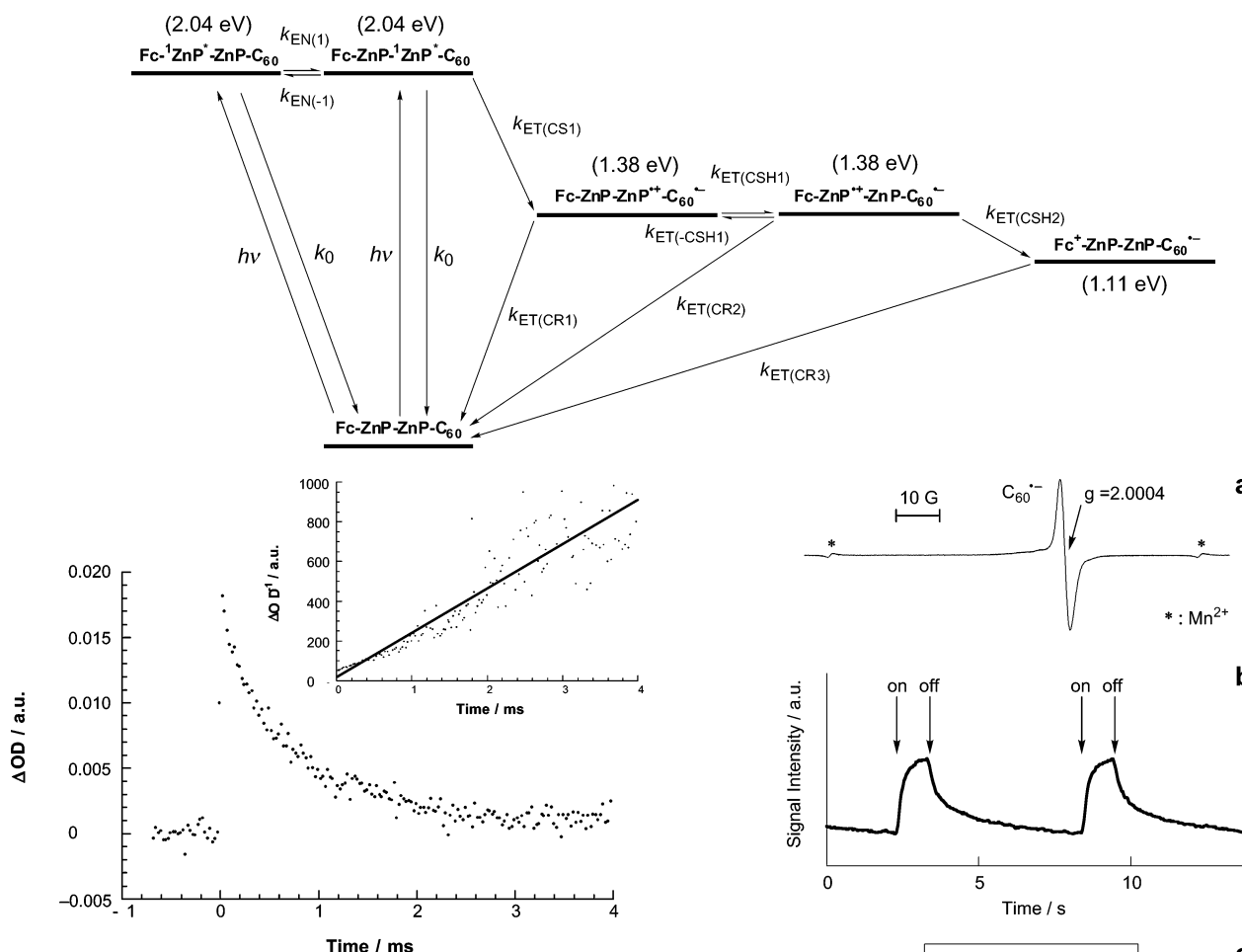
SCHEME 1

Figure 6. Time profile of absorbance at 1000 nm obtained by nanosecond time-resolved absorption spectra of the Fc−ZnP−ZnP−C_{60} tetrad in N_2-saturated DMF excited at 532 nm at 298 K. Inset: Second-order plot derived from the absorption change at 1000 nm.

2.3 G) is also typical for a derivatized $C_{60}^{\bullet-}$ with a low symmetry.[30] Since there is no significant broadening of the ESR signal, the spin−spin interaction in $Fc^+-ZnP-ZnP-C_{60}^{\bullet-}$ may be negligible because of the long distance between the Fc^+ and $C_{60}^{\bullet-}$ moieties. No direct ESR evidence for the ferricenium ion, Fc^+, in the $Fc^+-ZnP-ZnP-C_{60}^{\bullet-}$ pair is seen, which is rationalized by the well-known line-broadening of the Fc^+ ESR signal.[9] Thus, the observed ESR signal is virtually the same as that reported for $Fc^+-ZnP-H_2P-C_{60}^{\bullet-}$.[9] It should be emphasized that similar ESR signals are observed for $ZnP-C_{60}$ and $ZnP-H_2P-C_{60}$ under the same experimental conditions, but that the ESR intensities are negligibly small as compared with those of $Fc^+-ZnP-ZnP-C_{60}^{\bullet-}$.[9]

The ESR signal was monitored at a constant magnetic field. As shown in Figure 7b, an immediate growth of the ESR signal in frozen DMF was registered upon "turning on" the irradiation of $Fc-ZnP-ZnP-C_{60}$. During the illumination, only a slight amplification was noted. However, upon "turning off" the irradiation source, the ESR signal did not diminish instantaneously. Instead, a two-component decay was found (Figure 7c): A major, slow component that was best fitted by first-order kinetics yields a rate constant of 0.64 s^{-1} (corresponding to a lifetime of 1.6 s) which is assigned to the intramolecular charge-recombination process ($k_{ET(CR3)}$). A minor, fast component suggests the involvement of intermolecular electron transfer between two $Fc^+-ZnP-ZnP-C_{60}^{\bullet-}$ molecules. Similar behav-
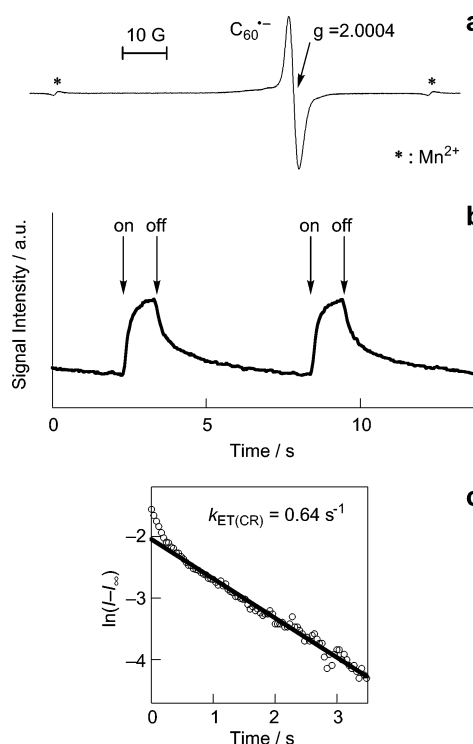

Figure 7. (a) ESR spectrum of $Fc-ZnP-ZnP-C_{60}$ $(1.0 \times 10^{-5}$ M) in a frozen deaerated DMF solution observed at 163 K under irradiation of ultraviolet−visible light from a high-pressure Hg lamp, (b) signal intensity response of $Fc^+-ZnP-ZnP-C_{60}^{\bullet-}$ $(1.0 \times 10^{-5}$ M) in a frozen deaerated DMF solution at the maximum of the ESR signal intensity due to the $C_{60}^{\bullet-}$, and (c) first-order plot for the decay of the ESR signal intensity (I) in $Fc-ZnP-ZnP-C_{60}$ ($k_{ET(CR)} = 0.64$ s^{-1}).

ior was noted for frozen PhCN, from which we determined a lifetime of 1.3 s at 163 K.[31]

Analysis of the electron-transfer reactions was carried out with the help of the Marcus equations (eqs 3 and 4),[20]

$$k_{ET} = \left(\frac{4\pi^3}{h^2\lambda k_B T}\right)^{1/2} V^2 \exp\left[-\frac{(\Delta G°_{ET} + \lambda)^2}{4\lambda k_B T}\right] \quad (3)$$

$$\Delta G^{\ddagger} = \frac{(\Delta G°_{ET} + \lambda)^2}{4\lambda} \quad (4)$$

with λ being the reorganization energy, $\Delta G°_{ET}$ the free energy change, V the electronic coupling matrix element, T the absolute temperature, and $\Delta G^{\ddagger}$ the activation barrier for the electron-
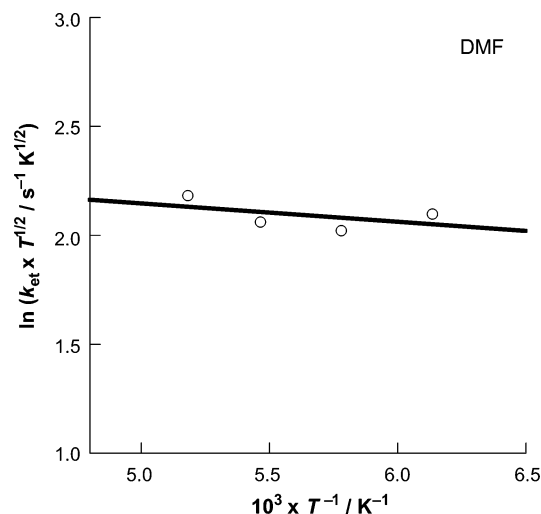
Molecular Tetrad Allowing Energy Storage for 1.6 s

J. Phys. Chem. A, Vol. 108, No. 4, 2004 **547**

Figure 8. Marcus analyses of the temperature dependence of $k_{ET(CR3)}$ for Fc–ZnP–ZnP–C_{60} in frozen DMF. The plot of $\ln(k_{ET(CR3)}T^{1/2})$ vs T^{-1} gave a straight line with the intercept (2.57) and the slope (0.0849) according to eq 5.

transfer reaction. Transformation of the "Marcus equation" (eq 3) into its linear form—as given in eq 5—enabled evaluation of $\Delta G^{\ddagger}$, λ, and V (vide infra).

$$\ln(k_{ET}T^{1/2}) = \ln\left(\frac{2\pi^{3/2}V^2}{h(\lambda k_B)^{1/2}}\right) - \frac{(\Delta G^{\circ}_{ET} + \lambda)^2}{4\lambda k_B T} \quad (5)$$

It should be mentioned that a plot of $\ln(k_{ET(CR3)}T^{1/2})$ vs T^{-1} reveals a small activation barrier ($\Delta G^{\ddagger}$), from which we derive an upper limit of 0.008 eV (Figure 8).[31] Such a weak temperature dependence is in accord with that observed for Fc$^+$–ZnP–H$_2$P–$C_{60}^{\bullet-}$.[9] On the basis of the weak temperature dependence, we rule out a stepwise intramolecular charge recombination via the Fc–ZnP$^{\bullet+}$–ZnP–$C_{60}^{\bullet-}$ and Fc–ZnP–ZnP$^{\bullet+}$–$C_{60}^{\bullet-}$ transients. The lifetime of the charge-separated state of Fc–ZnP–ZnP–C_{60} due to the intramolecular charge recombination at 298 K was determined from Figure 8 as 1.3 s in DMF. The reorganization energy (λ) and the electronic coupling matrix element (V) were determined as 1.16 eV and 5.6×10^{-5} cm^{-1} in DMF. The λ value of Fc$^+$–ZnP–ZnP–$C_{60}^{\bullet-}$ is similar to that of Fc$^+$–ZnP–H$_2$P–$C_{60}^{\bullet-}$ ($\lambda = 1.27$ eV),[9] because the electron donor ($C_{60}^{\bullet-}$) and acceptor (Fc$^+$) moieties are the same in Fc$^+$–ZnP–ZnP–$C_{60}^{\bullet-}$ and Fc$^+$–ZnP–H$_2$P–$C_{60}^{\bullet-}$. In contrast, the V value of Fc$^+$–ZnP–ZnP–$C_{60}^{\bullet-}$ is significantly smaller than the value of Fc$^+$–ZnP–H$_2$P–$C_{60}^{\bullet-}$ ($V = 1.9 \times 10^{-4}$ cm^{-1}). Such a smaller V value may result from the smaller orbital overlap between ZnP and $C_{60}^{\bullet-}$ in Fc$^+$–ZnP–ZnP–$C_{60}^{\bullet-}$ compared with that between H$_2$P and $C_{60}^{\bullet-}$ in Fc$^+$–ZnP–H$_2$P–$C_{60}^{\bullet-}$, because of the higher LUMO level (lower E°_{red}) of ZnP compared to H$_2$P (vide supra).

As far as the quantum yields regarding the conversion of photoexcited Fc–ZnP–ZnP–C_{60} into Fc$^+$–ZnP–ZnP–$C_{60}^{\bullet-}$ are concerned, by means of the comparative method (see the Experimental Section) we determined quantum yields that vary between 0.24 and 0.34; see Table 3. Relative to the Fc–ZnP–H$_2$P–C_{60} analogue, this is an amplification of about 40%.

Conclusions

In summary, in the current work we demonstrated the very slow intramolecular charge-recombination process (i.e., 1.3 s in DMF at 298 K by estimation from the temperature dependence, 1.6 s in DMF at 163 K, and 1.3 s in PhCN at 163 K)

within a novel molecular Fc–ZnP–ZnP–C_{60} tetrad, observable by ESR measurements under irradiation. Both the lifetime and the quantum yield of the final charge-separated state are improved in Fc–ZnP–ZnP–C_{60} relative to Fc–ZnP–H$_2$P–C_{60}. It should be emphasized here that the lifetime—1.3 s in DMF at 298 K—is by far the longest value ever reported for intramolecular charge recombination in synthetic donor–acceptor systems, including porphyrin–fullerene linked systems.[1–10,32,33] This value is also comparable to the lifetime ($\sim$1 s) of the bacteriochlorophyll dimer radical cation ((Bchl)$_2^{\bullet+}$)–secondary quinone radical anion (Q$_B^{\bullet-}$) ion pair in bacterial photosynthetic reaction centers.[8]

References and Notes

(1) (a) Meyer, T. J. *Acc. Chem. Res.* **1989**, *22*, 163. (b) Wasielewski, M. R. *Chem. Rev.* **1992**, *92*, 435. (c) Paddon-Row, M. N. *Acc. Chem. Res.* **1994**, *27*, 18. (d) Jordan, K. D.; Paddon-Row, M. N. *Chem. Rev.* **1992**, *92*, 395.

(2) (a) Kurreck, H.; Huber, M. *Angew. Chem., Int. Ed. Engl.* **1995**, *34*, 849. (b) Harriman, A.; Sauvage, J.-P. *Chem. Soc. Rev.* **1996**, *26*, 41. (c) Blanco, M.-J.; Jiménez, M. C.; Chambron, J.-C.; Heitz, V.; Linke, M.; Sauvage, J.-P. *Chem. Soc. Rev.* **1999**, *28*, 293.

(3) (a) Balzani, V.; Juris, A.; Venturi, M.; Campagna, S.; Serroni, S. *Chem. Rev.* **1996**, *96*, 759. (b) Osuka, A.; Mataga, N.; Okada, T. *Pure Appl. Chem.* **1997**, *69*, 797.

(4) (a) Gust, D.; Moore, T. A.; Moore, A. L. *Acc. Chem. Res.* **1993**, *26*, 198. (b) Gust, D.; Moore, T. A.; Moore, A. L. *Acc. Chem. Res.* **2001**, *34*, 40.

(5) Verhoeven, J. W. *Adv. Chem. Phys.* **1999**, *106*, 603.

(6) (a) Imahori, H.; Sakata, Y. *Adv. Mater.* **1997**, *9*, 537. (b) Imahori, H.; Sakata, Y. *Eur. J. Org. Chem.* **1999**, *2445*, 5. (c) Imahori, H.; Fukuzumi, S. *Adv. Mater.* **2001**, *13*, 1197. (d) Imahori, H.; Mori, Y.; Matano, Y. *J. Photochem. Photobiol., C* **2003**, *4*, 51.

(7) (a) Fukuzumi, S.; Imahori, H. In *Electron Transfer in Chemistry*; Balzani, V., Ed.; Wiley-VCH: Weinheim, Germany, 2001; Vol. 2, pp 927–975. (b) Fukuzumi, S.; Guldi, D. M. In *Electron Transfer in Chemistry*; Balzani, V., Ed.; Wiley-VCH: Weinheim, Germany, 2001; Vol. 2, pp 270–337.

(8) (a) *The Photosynthetic Reaction Center*; Deisenhofer, J., Norris, J. R., Eds.; Academic Press: San Diego, 1993. (b) *Anoxygenic Photosynthetic Bacteria*; Blankenship, R. E., Madigan, M. T., Bauer, C. E., Eds.; Kluwer Academic Publishing: Dordrecht, The Netherlands, 1995.

(9) Imahori, H.; Guldi, D. M.; Tamaki, K.; Yoshida, Y.; Luo, C.; Sakata, Y.; Fukuzumi, S. *J. Am. Chem. Soc.* **2001**, *123*, 6617.

(10) (a) Imahori, H.; Hagiwara, K.; Akiyama, T.; Aoki, S.; Taniguchi, M.; Okada, T.; Shirakawa, M.; Sakata, Y. *Chem. Phys. Lett.* **1996**, *263*, 545. (b) Imahori, H.; Tkachenko, N. V.; Vehmanen, V.; Tamaki, K.; Lemmetyinen, H.; Sakata, Y.; Fukuzumi, S. *J. Phys. Chem. A* **2001**, *105*, 1750. (c) Imahori, H.; Yamada, H.; Guldi, D. M.; Endo, Y.; Shimomura, A.; Kundu, S.; Yamada, K.; Okada, T.; Sakata, Y.; Fukuzumi, S. *Angew. Chem., Int. Ed.* **2002**, *41*, 2344.

(11) (a) Prato, M. *J. Mater. Chem.* **1997**, *7*, 1097. (b) Martín, N.; Sánchez, L.; Illescas, B.; Pérez, I. *Chem. Rev.* **1998**, *98*, 2527. (c) Diederich, F.; Gomez-Lopez, M. *Chem. Soc. Rev.* **1999**, *28*, 263. (d) Guldi, D. M. *Chem. Commun.* **2000**, 321.

(12) Leading examples: (a) Imahori, H.; Hagiwara, K.; Aoki, M.; Akiyama, T.; Taniguchi, S.; Okada, T.; Shirakawa, M.; Sakata, Y. *J. Am. Chem. Soc.* **1996**, *118*, 11771. (b) Imahori, H.; Norieda, H.; Yamada, H.; Nishimura, Y.; Yamazaki, I.; Sakata, Y.; Fukuzumi, S. *J. Am. Chem. Soc.* **2001**, *123*, 100.

(13) Leading examples: (a) Liddell, P. A.; Kuciauskas, D.; Sumida, J. P.; Nash, B.; Nguyen, D.; Moore, A. L.; Moore, T. A.; Gust, D. *J. Am. Chem. Soc.* **1997**, *119*, 1400. (b) Kuciauskas, D.; Liddell, P. A.; Lin, S.; Johnson, T. E.; Weghorn, S. J.; Lindsey, J. S.; Moore, A. L.; Moore, T. A.; Gust, D. *J. Am. Chem. Soc.* **1999**, *121*, 8604.

(14) Leading examples: (a) Armaroli, N.; Diederich, F.; Dietrich-Buchecker, C. O.; Flamigni, L.; Marconi, G.; Nierengarten, J.-F.; Sauvage, J.-P. *Chem.—Eur. J.* **1998**, *4*, 406. (b) Nierengarten, J.-F.; Schall, C.; Nicoud, J.-F.; *Angew. Chem., Int. Ed.* **1998**, *37*, 1934.

(15) Leading examples: (a) Baran, P. S.; Monaco, R. R.; Khan, A. U.; Schuster, D. I.; Wilson, S. R. *J. Am. Chem. Soc.* **1997**, *119*, 8363. (b) Schuster, D. I.; Cheng, P.; Wilson, S. R.; Prokhorenko, V.; Katterle, M.; Holzwarth, A. R.; Braslavsky, S. E.; Klihm, G.; Williams, R. M.; Luo, C. *J. Am. Chem. Soc.* **1999**, *121*, 11599.

(16) Leading examples: (a) Tkachenko, N. V.; Rantala, L.; Tauber, A. Y.; Helaja, J.; Hynninen, P. H.; Lemmetyinen, H. *J. Am. Chem. Soc.* **1999**, *121*, 9378. (b) Tkachenko, N. V.; Vuorimaa, E.; Kesti, T.; Alekseev, A. S.; Tauber, A. Y.; Hynninen, P. H.; Lemmetyinen, H. *J. Phys. Chem. B* **2000**, *104*, 6371.

(17) Leading examples: (a) Bell, T. D. M.; Smith, T. A.; Ghiggino, K. P.; Ranasinghe, M. G.; Shephard, M. J.; Paddon-Row, M. N. *Chem. Phys. Lett.* **1997**, *268*, 223. (b) Bell, T. D. M.; Ghiggino, K. P.; Jolliffe, K. A.; Ranasinghe, M. G.; Langford, S. J.; Shephard, M. J.; Paddon-Row, M. N. *J. Phys. Chem. A* **2002**, *106*, 10079.

(18) Leading example: (a) Montforts, F.-P.; Kutzki, O. *Angew. Chem., Int. Ed.* **2000**, *39*, 599. (b) Smirnov, S.; Vlassiouk, I.; Kutzki, O.; Wedel, M.; Montforts, F.-P. *J. Am. Chem. Soc.* **2002**, *124*, 4212.

(19) Leading examples: (a) D'Souza, F.; Deviprasad, G. R.; Rahman, M. S.; Choi, J.-P. *Inorg. Chem.* **1999**, *38*, 2157. (b) D'Souza, F.; Deviprasad, G. R.; El-Khouly, M. E.; Fujitsuka, M.; Ito, O. *J. Am. Chem. Soc.* **2001**, *123*, 5277.

(20) (a) Marcus, R. A. *Angew. Chem., Int. Ed. Engl.* **1993**, *32*, 1111. (b) Winkler, J. R.; Gray, H. B. *Chem. Rev.* **1992**, *92*, 369. (c) Newton, M. D. *Chem. Rev.* **1991**, *91*, 767.

(21) Imahori, H.; Tamaki, K.; Guldi, D. M.; Luo, C.; Fujitsuka, M.; Ito, O.; Sakata, Y.; Fukuzumi, S. *J. Am. Chem. Soc.* **2001**, *123*, 2607.

(22) Luo, C.; Guldi, D. M.; Imahori, H.; Tamaki, K.; Sakata, Y. *J. Am. Chem. Soc.* **2000**, *122*, 6535.

(23) Guldi, D. M.; Prato, M. *Acc. Chem. Res.* **2000**, *33*, 695.

(24) Guldi, D. M.; Kamat, P. V. In *Fullerenes Chemistry, Physics, and Technology*; Kadish, K. M., Ruff R. S., Eds.; Wiley-Interscience: New York, 2000; pp 225−281.

(25) It was however impossible to find grounds for analyzing the charge-shift reactions between the two zinc porphyrins.

(26) Since the two zinc porphyrins differ only marginally in terms of their redox behavior, the lack of driving force suppresses the secondary electron transfer to a large or even exclusive extent. In fact, determining the quantum yields of charge separation for the two radical ion pairs, namely, $ZnP-ZnP^{\bullet+}-C_{60}^{\bullet-}$ and $ZnP^{\bullet+}-ZnP-C_{60}^{\bullet-}$, supported the fact that the distant and long-lived radical ion pair is formed in minor yields (ca. 7%).

(27) Alternatively, a quantum mechanical mechanism should be considered ($\Psi_{\pm} = 1/\sqrt{2}\ [\psi(ZnP-ZnP^{\bullet+}-C_{60}^{\bullet-}) \pm \psi\ (ZnP^{\bullet+}-ZnP-C_{60}^{\bullet-})]$), in which the two states, that is, the symmetric and asymmetric combination, might be closer to stationary states of the $ZnP-ZnP-C_{60}$ triad.

(28) (a) Imahori, H.; Tamaki, K.; Araki, Y.; Sekiguchi, Y.; Ito, O.; Sakata, Y.; Fukuzumi, S. *J. Am. Chem. Soc.* **2002**, *124*, 5165. (b) Fukuzumi, S.; Okamoto, K.; Yoshida, Y.; Imahori, H.; Araki, Y.; Ito, O. *J. Am. Chem. Soc.* **2003**, *124*, 1007.

(29) Further evidence for the second-order rate law stemmed from changing the effective radical ion pair concentration via employing different laser powers over a wide range (i.e., increments to reach a 5-fold increase in laser intensity) and also by changing the initial $Fc-ZnP-ZnP-C_{60}$ concentration (i.e., $(2.0-20) \times 10^{-6}$ M).

(30) (a) Fukuzumi, S.; Mori, H.; Suenobu, T.; Imahori, H.; Gao, X.; Kadish, K. M. *J. Phys. Chem. A* **2000**, *104*, 10688. (b) Fukuzumi, S.; Suenobu, T.; Gao, X.; Kadish, K. M. *J. Phys. Chem. A* **2000**, *104*, 2908.

(31) It should be noted that the CR driving force in the frozen matrix may be larger than the value in solution. However, the observation of the charge-separated state rather than the triplet excited state of C_{60} or ZnP indicates that the CR driving force should be smaller than the triplet energies of C_{60} and ZnP as the case in solution. The energies of the charge-separated states of fullerene-based systems are less sensitive to changes in solvent dielectric constant and environment (i.e., rigid matrix) relative to those for similar molecules with quinone electron acceptors. See: Kuciauskas, D.; Liddell, P. A.; Lin, S.; Stone, S. G.; Moore, A. L.; Moore, T. A.; Gust, D. *J. Phys. Chem. B* **2000**, *104*, 4307.

(32) (a) Gust, D.; Niemczyk, M.; Moore, T. A.; Moore, A. L.; Macpherson, A. N.; Lopez, A.; DeGraziano, J. M.; Gouni, I.; Bittersmann, E.; Seely, G. R.; Gao, F.; Nieman, R. A.; Ma, X. C.; Demanche, L. J.; Hung, S.-C.; Luttrull, D. K.; Lee, S.-J.; Kerrigan, P. K. *J. Am. Chem. Soc.* **1993**, *115*, 11141. (b) Wasielewski, M. R.; Gains, G. L.; Wiederrecht, G. P.; Svec, W. A.; P. *J. Am. Chem. Soc.* **1993**, *115*, 10442.

(33) (a) Fukuzumi, S.; Ohkubo, K.; Imahori, H.; Shao, J.; Ou, Z.; Zheng, G.; Chen, Y.; Pandey, R. K.; Fujitsuka, M.; Ito, O.; Kadish, K. M. *J. Am. Chem. Soc.* **2001**, *123*, 10676. (b) Hu, Y.-Z.; Tsukiji, S.; Shinkai, S.; Oishi, S.; Hamachi, I. *J. Am. Chem. Soc.* **2000**, *122*, 241. (c) Kashiwagi, Y.; Ohkubo, K.; McDonald, J. A.; Blake, I. M.; Crossley, M. J.; Araki, Y.; Ito, O.; Imahori, H.; Fukuzumi, S. *Org. Lett.* **2003**, *5*, 2719.